Dielectric properties of ZrN, NbC, and NbN as determined by electron-energy-loss spectroscopy

J. Pflüger,* J. Fink, W. Weber, and K.-P. Bohnen
Kernforschungszentrum Karlsruhe, Institut für Nukleare Festkörperphysik, Postfach 3640, D-7500 Karlsruhe, Federal Republic of Germany

G. Crecelius
Institut für Festkörperforschung der Kernforschungsanlage Jülich, Postfach 1913, D-5170 Jülich, Federal Republic of Germany

(Received 2 July 1984)

The dielectric properties of ZrN, NbC, and NbN in the energy range from 1.5 to about 38 eV were determined using high-resolution, high-energy electron-energy-loss spectroscopy. The Kramers-Kronig–derived optical joint densities of states agree well with calculated joint densities of states for NbC and ZrN. The results are compared to the corresponding $3d$ compounds.

I. INTRODUCTION

ZrN, NbC, and NbN belong to the group of refractory compounds which exhibit a number of exceptional physical properties,[1,2] such as high melting points, great hardness, brittleness, and superconductivity, which are closely related to their electronic structure.[3–7]

The work presented here is an extension of an electron-energy-loss (EELS) study of the $3d$ refractory compounds TiC, TiN, VC, and VN.[8,9] With the exception of ZrN, where optical data up to 12 eV have been published,[10] neither optical nor high-energy EELS data exist for these materials. The purpose of this paper therefore is to provide experimental data and to compare these with band-structure calculations.

II. EXPERIMENTAL

The samples for this work were prepared by reactive sputtering. The preparation is described in more detail in Refs. 8 and 9.

For characterization and analysis, the samples were investigated by means of thin-film x-ray diffraction, Rutherford backscattering, a $^{12}C^{13}(d,p)$ nuclear reaction method,[11] and transmission-electron microscopy. In addition, the transition temperature to superconductivity (T_c) was measured with an inductive method. T_c is very sensitive to nonmetal vacancies and to oxygen contamination. Parameters characterizing the samples are summarized in Table I.

Lattice parameters of all compounds were in agreement with the nonmetal-to-metal ratio determined with the ion-beam techniques. Also, the T_c values of NbC and NbN indicate a nonmetal-to-metal ratio close to 1.[1] ZrN did not show a T_c down to 4.2 K, which was attributed to an oxygen contamination of (7 ± 5) at. %. Because of its complicated phase diagram, NbN was difficult to prepare in the pure fcc phase. The x-ray diffraction patterns of some samples showed very weak lines which belonged to different crystal structures. In the x-ray spectra of ZrN and NbC only fcc lines were present.

The 170 keV electron-energy-loss spectrometer used for this investigation is described in more detail in Ref. 8. For the measurements presented here it was operated at an energy resolution of 0.1 eV and a momentum resolution between 0.04 and 0.08 Å^{-1}.

III. LOSS FUNCTIONS

The loss functions $\mathrm{Im}(-1/\epsilon)$ of ZrN, NbC, and NbN are shown in Fig. 1 by the solid lines. These functions were obtained directly from the measured raw data in the following way: First, the elastic line was subtracted. Second, a numerical deconvolution to correct for finite spectrometer resolution and double scattering was applied. Third, the data were normalized. The real and imaginary parts of the dielectric functions ϵ_1 and ϵ_2 which were obtained by a Kramers-Kronig analysis are also shown in Fig. 1 by the dot-dashed and dashed lines, respectively. For more details about the determination of the loss functions and the dielectric properties we refer to Refs. 8, 9, and 12.

The raw data were truncated at 36 eV for ZrN and at 38 eV for NbC and NbN. Above these energies, multiple energy losses were believed to influence the precision of the data. A comparison of the measured loss function with ϵ_1 and ϵ_2 shows that maxima in the loss functions are correlated with a zero or small absolute value of ϵ_1 and a small ϵ_2. The better this condition is fulfilled, the sharper and more pronounced the maximum in $\mathrm{Im}(-1/\epsilon)$. The dominant feature in all spectra is the plasmon found at 22.3, 24.0, and 25.3 eV for ZrN, NbC, and NbN, respectively. These values may be compared with the free-electron-plasma energy. Including the nonmetal $2s$ and $2p$ as well as the metal $4d$ and $5s$ orbitals we obtained 22.8, 23.6, and 25.5 eV for ZrN, NbC, and NbN, respectively, which is in quite good agreement with the measured values. Schubert *et al.*[13] obtained 21.5 and 24.0 eV for $ZrN_{0.72}$ and $NbN_{0.8}$, respectively, using EELS in

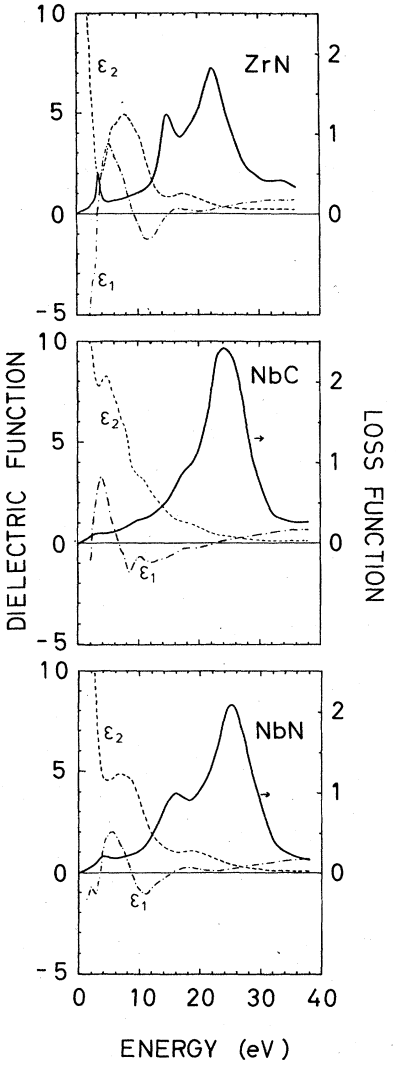

FIG. 1. Loss functions (solid lines), Kramers-Kronig–derived real and imaginary parts of the dielectric function (dot-dashed and dashed, respectively).

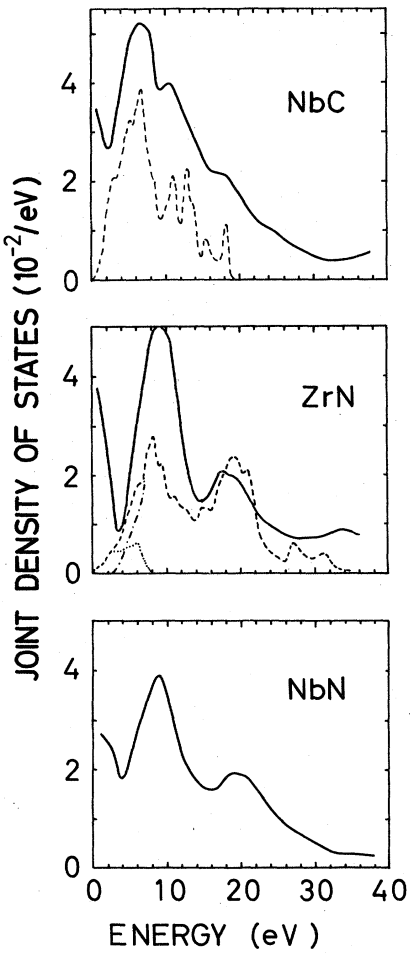

FIG. 2. Optical joint density of states (solid lines) and joint densities of states, calculated from band-structure data (dashed lines). In ZrN, the JDS function for d-d transitions (dotted) and the JDS function without d-d transitions (dotted-dashed) were also calculated.

reflection. Their smaller values may be a result of their substoichiometric samples. In the isoelectronic $3d$ compounds TiN, VC, and VN, the same close relationship to the free-electron-plasma energy was observed.[8] A characteristic low energy plasma loss ($\epsilon_1=0$) is found at 3.6, 2.9, and 3.9 eV in ZrN, NbC, and NbN, respectively. It is quite sharp and pronounced in ZrN but broadened and damped in NbC and NbN. In the $3d$ compounds TiN and VN, these losses showed the same shapes but were found at somewhat lower energies.[8] $VC_{0.88}$ did not exhibit the low-energy plasmon. Its absence in comparison with the NbC spectrum was attributed to vacancy effects in $VC_{0.88}$. In the $3d$ compounds the formation of this loss was explained in a simple Drude-Lorentz model.[8] It was shown to be the Drude plasmon which is shifted down by strong interband transitions at higher energies. The stronger damping of this plasmon in NbC and NbN is due to interband absorption and to a larger Drude damping constant. Above 15 eV only one maximum is visible in the nitride spectra, which is caused by strong interband transitions around 19 eV and will be discussed in the next section. In this energy range, some differences were visible as compared to the corresponding $3d$ compound where two maxima were observed.

IV. OPTICAL JOINT DENSITIES OF STATES AND COMPARISON WITH BAND-STRUCTURE DATA

The optical joint density of states (OJDS) can be defined as[14]

$$J_1(E)=\frac{E\epsilon_2(E)}{(\pi/2)E_p^2},$$

where E_p is the free-electron-plasma energy. The OJDS curves derived by a Kramers-Kronig analysis of the loss functions are shown in Fig. 2 by the solid lines. The dashed lines in the NbC and ZrN curves are joint densities of states (JDS) calculated from a tight-binding fit of Weber[15] to the augmented-plane-wave results of Schwarz[5] in the case of NbC and from self-consistent Gaussian

TABLE I. Results of sample analysis.

	Thickness (Å)	a_0 (Å)	T_c (K)	nonmetal-metal ratio	oxygen contamination (at. %)
ZrN	1100	4.574±0.002	<4.2	1.0±0.05	7±5
NbC	1300	4.476±0.003	9.5	1.0±0.05	
NbN	920	4.394±0.004	15.5	1.0±0.05	<3

LCAO data in the case of ZrN. The JDS neglect matrix elements and give an approximation to the interband contribution to the OJDS.

At energies up to about 2.5 eV the OJDS is dominated by intraband transitions in all compounds. In ZrN the interband contribution up to 3 eV is quite low, which is evident from the deep minimum in the spectrum. In this case the Drude plasma energy E_{p0} and damping constant Γ_0 can be estimated (see Ref. 8). We obtained 8.8 eV for E_{p0} and 2.2 eV for Γ_0. The reason for the low interband damping in ZrN at these energies is obviously the same as in TiN.[8] The Fermi level lies within the d bands where only very few p states are available.[16] Because transitions between pure d states localized at the metal atoms are dipole forbidden, no interband damping occurs at low energies. To emphasize this we calculated the d-d contribution to the JDS (dotted curve in the ZrN spectrum in Fig. 2). The JDS without these d-d transitions (dot-dashed curve) sets in at about 3 eV and is also quite small at 3.3 eV where the shifted Drude plasmon is observed.

In NbC and NbN the p-like density of states around the Fermi energy is considerably larger than in ZrN. Thus more interband transitions are possible at low energies and an additional damping mechanism for the Drude plasmon is provided. The low-energy plasma excitations in TiN and VN followed exactly the same trends.[8]

At higher energies, the curves in Fig. 2 are dominated by interband transitions only. The broad peak around 8—10 eV in all compounds corresponds to strong transitions between p and d bands which are reproduced quite well by the JDS. The peaks at 10 eV in NbC and 18 eV in ZrN can be assigned to transitions from nonmetal s bands to the lower part of the d bands. The shoulder at 18 eV in NbC is caused by C $2s$ transitions to unoccupied d-derived states several eV above the Fermi level. Very similar transitions were observed in the corresponding $3d$ compounds.[8] Structures above 25 eV must be attributed to transitions to bands above the d bands. Also the Zr $4p$ core excitation becomes possible at about 30 eV which was not included in our calculations.

The peak positions of the experimental OJDS curves and the theoretical JDS results agree well. However, the JDS curves show more structure than the experimental data; this is most probably due to lifetime effects which have not been included in the theory. Also the relative peak amplitudes are not correctly reproduced, because of matrix-element effects which have also been neglected.

As compared to $VC_{0.88}$ the OJDS of NbC shows a clear minimum around 3 eV. As already mentioned this difference has its origin in an increased transition rate in $VC_{0.88}$ due to nonmetal vacancies which enhances the OJDS and damps out the low-energy plasma excitation. Above 12 eV the OJDS of the $3d$ and $4d$ compounds show some differences. The $2s$-d transitions in NbC are less pronounced than in $VC_{0.88}$. In the $3d$ nitrides, a peak at 12 eV, arising from transitions between p bands and states above the d bands, was observed which is not present in ZrN and NbN. In the $4d$ compounds, the p as well as the d bands are somewhat broader as compared to the $3d$ materials. Therefore the broad p-d transitions peak in the OJDS centered around 10 eV extends to higher energies. Thus transitions to states above the d bands around 12 eV might be obscured.

V. SUMMARY

NbC, ZrN, and NbN were studied using high-resolution electron-energy-loss spectroscopy. The loss functions, as well as the Kramers-Kronig—derived dielectric properties showed some similarity as well as characteristic differences to the related $3d$ compounds. In all spectra, a characteristic low-energy loss around 3.5 eV was observed. The damping mechanism for this loss was shown to be the same as for the corresponding $3d$ materials. The main volume plasma loss was observed near the free-electron plasma energy. The optical joint densities of states derived from these data were compared to joint densities of states deduced from band-structure data. The agreement was quite well. Differences in the corresponding $3d$ compounds can be explained by different band structures.

ACKNOWLEDGMENTS

The authors would like to thank R. von Baltz for helpful discussions and W. Schmatz and M. Campagna for continued support. We are indepted to G. Linker, R. Kaufmann, and F. Wüchner for carrying out some of the Rutherford backscattering measurements.

*Present address: Institut für Festkörperforschung der Kernforschungsanlage Jülich, Postfach 1913, D-5170 Jülich, Federal Republic of Germany.

[1]L. E. Toth, *The Transition Metal Carbides and Nitrides* (Academic, New York, 1971).

[2]E. K. Storms, *The Refractory Carbides* (Academic, New York, 1967).

[3]J. L. Calais, Adv. Phys. **26**, 847 (1977).

[4]A. Neckel, Int. J. Quantum Chem. **23**, 1317 (1983).

[5]K. Schwarz, J. Phys. C **10**, 195 (1977).

[6]K. Schwarz, J. Phys. C **8**, 809 (1975).
[7]K. Schwarz, H. Ripplinger, and A. Neckel, Z. Phys. B **48**, 79 (1982).
[8]J. Pflüger, J. Fink, W. Weber, K.-P. Bohnen, and G. Crecelius, Phys. Rev. B **30**, 1155 (1984).
[9]J. Pflüger, Ph.D. thesis, University of Karlsruhe, 1983, also obtainable from the Kernforschungszentrum Karlsruhe (KfK) Report No. 3585 (in German) (unpublished).
[10]A. Schlegel, P. Wachter, J. J. Nikkl, and H. Lingg, J. Phys. C **10**, 4889 (1977).
[11]*Ion Beam Handbook For Material Analysis,* edited by J. W. Mayer and E. Rimini (Academic, New York, 1977).
[12]J. Daniels, C. Festenberg, H. Raether, and K. Zeppenfeld, in *Optical Constants of Solids by Electron Spectroscopy,* Vol. 54 of *Springer Tracts in Modern Physics,* edited by G. Höhler (Springer, New York, 1970), p. 77.
[13]W. K. Schubert, R. N. Shelton, and E. L. Wolf, Phys. Rev. B **24**, 6278 (1981).
[14]W. Y. Liang and A. R. Beal, J. Phys. C **9**, 2823 (1976).
[15]W. Weber, in *Electronic Structure of Complex Systems,* edited by W. Temmermann and P. Phariseau (Plenum, New York, 1983).
[16]R. Eibler, M. Dorrer, and A. Neckel, Theor. Chim. Acta. **63**, 133 (1983).